ACS OMEGA

Open Access

http://pubs.acs.org/journal/acsodf

Article

Advancing Ionic Liquid Research with pSCNN: A Novel Approach for Accurate Normal Melting Temperature Predictions

Tao Liang, Wei Liu, Kai Tan, Anan Wu,* and Xin Lu*

Cite This: *ACS Omega* 2024, 9, 31694−31702

Read Online

ACCESS | Metrics & More | Article Recommendations | Supporting Information

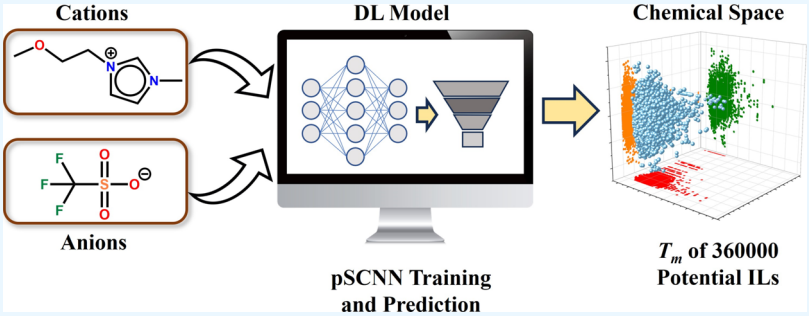

ABSTRACT: Ionic liquids (ILs), known for their distinct and tunable properties, offer a broad spectrum of potential applications across various fields, including chemistry, materials science, and energy storage. However, practical applications of ILs are often limited by their unfavorable physicochemical properties. Experimental screening becomes impractical due to the vast number of potential IL combinations. Therefore, the development of a robust and efficient model for predicting the IL properties is imperative. As the defining feature, it is of practice significance to establish an accurate yet efficient model to predict the normal melting point of IL (T_m), which may facilitate the discovery and design of novel ILs for specific applications. In this study, we presented a pseudo-Siamese convolution neural network (pSCNN) inspired by SCNN and focused on the T_m. Utilizing a data set of 3098 ILs, we systematically assess various deep learning models (ANN, pSCNN, and Transformer-CNF), along with molecular descriptors (ECFP fingerprint and Mordred properties), for their performance in predicting the T_m of ILs. Remarkably, among the investigated modeling schemes, the pSCNN, coupled with filtered Mordred descriptors, demonstrates superior performance, yielding mean absolute error (MAE) and root-mean-square error (RMSE) values of 24.36 and 31.56 °C, respectively. Feature analysis further highlights the effectiveness of the pSCNN model. Moreover, the pSCNN method, with a pair of inputs, can be extended beyond ionic liquid melting point prediction.

1. INTRODUCTION

Ionic liquids (ILs) are a class of liquids composed entirely of organic cations and inorganic/organic anions, which are typically in liquid state at temperatures below 100 °C.[1] The unique chemical composition imparts various essential properties to ILs, including low volatility, high thermal stability, a wide liquid range, nonflammability, and high ionic conductivity.[1] Consequently, ILs have recently attracted increasing and broad interest from both academia and industry.[2−10] The distinctive chemical composition also bestows upon ionic liquids a crucial characteristic: the ability to tailor their physical, chemical, and biological properties to address specific challenges through modifications to the corresponding cations and/or anions. For example, the normal melting temperature (T_m) of methanaminium bromide can be systematically reduced from 237 to 111 and 13 °C by replacing bromide with nitrate and formate anions, respectively.[11] Despite significant advances in synthetic chemistry that have accelerated IL production, the experimental screening of ILs remains impractical due to the vast number of potential combinations of organic cations and inorganic/organic anions.[12]

To tune the properties of ILs from a theoretical perspective, a profound understanding of the molecular structure and thermodynamics governing the ionic liquid system is necessary. Ab initio molecular dynamics and quantum chemical calculations offer a route to obtain reliable results,[13] although these calculations are not feasible due to the prohibitive computational scaling of these methods. Quantitative structure−property relationship-based (QSPR) methods have been extensively employed to predict the physical and

Received: March 11, 2024
Revised: April 12, 2024
Accepted: June 25, 2024
Published: July 8, 2024

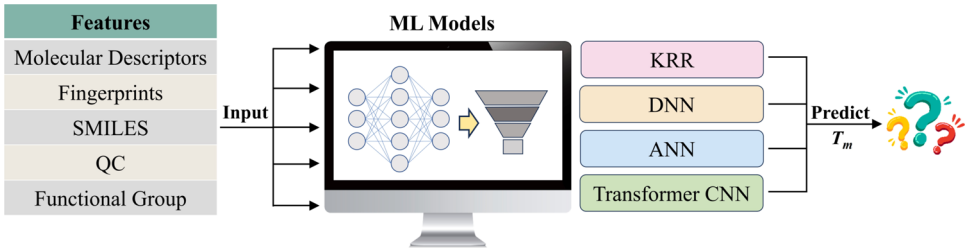

Figure 1. Various machine learning models for predicting the T_m of ionic liquids.

chemical properties of ILs and have achieved notable successes.[12,14−18] Among the various properties, T_m is of great importance as a defining feature. Katritzky et al. developed a QSPR model for a data set of 126 pyridinium bromides using 6 descriptors, achieving an accuracy with a square correlation coefficient (R^2) of 0.788.[12] Since then, numerous attempts have been made to construct accurate QSPR models for estimating the T_m of ILs and have achieved certain successes(Table S1).[14−18] However, several key factors have limited broad applications of these QSPR models: (1) QSPR-based models heavily depend on the quality and quantity of the data used for training. If the data set is limited or contains biases as in the case of previous investigations, the model's predictions may not be reliable for broader applications; (2) The choice of molecular descriptors is crucial for QSPR models. If the selected descriptors are not truly representative of the molecular features influencing the property of interest, the model may not perform well in the blind test; (3) QSPR models often assume a linear relationship between descriptors and properties. It has been shown that the melting process of ILs is complicated and the descriptors are generally not linearly correlated with the T_m of ILs.[19] Hence, more sophisticated methods are needed to better describe the correlation between the structure and the T_m values of ILs.

While tackling complex and nonlinear problems, modern machine learning methods (ML), supported by big data, have demonstrated superior efficiency and accuracy compared to traditional QSPR methods, achieving considerable success in predicting various properties of chemical materials.[20,21] Over the past few decades, numerous ML models have been developed to predict the T_m values of ILs (Figure 1). Early ML efforts primarily focused on predicting the T_m of specific types of ILs due to a lack of sufficiently diverse data,[22] and hence are lack of generalization capability in nature. Recently, Venkatraman et al.[23] carefully compiled a comprehensive data set of 2212 ILs from the literature, facilitating ML models with generalization capabilities. Regression analyses, employing various ML methods, yielded prediction R^2 values ranging from 0.53 to 0.67.[23] Notably, the classification models revealed better accuracy (84%) in discriminating between ILs with T_m higher than 100 °C and those below 100 °C. Utilizing the same data set, Low et al.[24] proposed a kernel ridge regression (KRR) model based on the extended connectivity fingerprint (ECFP4), Coulomb matrix, and molecular orbital energies derived from ab initio calculations, predicting the T_m of ILs with average mean absolute error (MAE), root-mean-square error (RMSE) and R^2 of 29, 45 °C, and 0.74, respectively. This model, in contrast to the group contribution methods and traditional QSPR methods, is applicable to any type of ionic liquid.

With the development of deep learning methods (DL), it is widely accepted that DL surpasses normal ML in handling complex and nonlinear problems. A benchmark investigation by Baskin et al.[25] indeed demonstrated that nonlinear MLs outperform traditional linear models, and DLs outperform MLs. Furthermore, the Transformer, actively utilized in natural language processing, may offer a promising alternative for modeling the physical properties of ILs. In a recent development, Makarov et al.[26,27] collected the largest and most comprehensive data set consisting of 3073 ILs. They utilized the Transformer Convolutional Neural Network (Transformer-CNN) equipped with a SMILES representation to predict the T_m of ILs. Two models, based on the whole data set, were developed with different cross-validation (CV) protocols (Component and Mixture). Reasonable accuracies have been achieved with R^2 of 0.66 and 0.78,[27] respectively. However, the generalization capability of these models needs further assessment due to the lack of sufficient external validation.

The T_m of ILs is controlled by both single-molecule properties and intermolecular interactions.[1,28] Therefore, an effective model for predicting the T_m of ILs must accurately describe not only the properties of anions and cations themselves but also capture the complex and nonlinear correlations between them. In the field of computer vision, a specialized architecture, the Siamese convolutional neural network (SCNN) is designed for tasks that involve assessing the similarity or dissimilarity between pairs of inputs. SCNN is constructed to learn and extract features from pairs of input samples, making decisions based on their similarity.[29] Compared to conventional artificial neural networks (ANNs) and Transformer-based methods, SCNNs focus on learning correlation between pair inputs and making predictions based on that. Consequently, they have demonstrated successful applications in image recognition,[30] natural product identification,[31] and bioactivity prediction.[32] These characteristics suggest that SCNN is particularly well suited to predict the T_m of ILs using pairwise inputs of anions and cations. In this contribution, a pseudo-Siamese convolution neural network (pSCNN), inspired by SCNN, was developed to predict the T_m of ILs.

2. METHODS

2.1. Data Set. To date, the most comprehensive data set, compiled by Makarov et al.,[27] comprises 3073 records. As new data keep on appearing in journals and monographs, this work endeavors to enhance the data set's comprehensiveness. Building upon the data set of Makarov et al.,[27] journal articles,[23] and NIST ILThermo database,[11] we complied a more extensive data set. Several protocols have been adopted to ensure a relatively low noise level. For instance, when multiple melting point values were reported for a given IL, the most recent measurement was selected under the assumption that the recent measurement is more accurate due to the

https://doi.org/10.1021/acsomega.4c02393
ACS Omega 2024, 9, 31694−31702

advances in experimental. In cases in which the melting point is presented as a range, the midpoint was adopted. Ionic liquids consisting of more than two types of ions were also excluded, aligning with the pSCNN's capability to process pairs of inputs. The resultant data set comprises the T_m of 3098 ILs, featuring 203 distinct anions and 1760 unique cations. The cleaned data set was imported as a DataFrame in Python using the pandas package,[33] serving as the foundation for various analyses and model selections in the subsequent sections.

Detailed analysis reveals that the T_m of 3098 ILs range from 177 to 592 K, with an average T_m of 357 K. Noted that the T_m distribution complies well with the standard normal distribution (Figure 2), suggesting the current data set is representative in terms of the T_m. However, further examination shows that majority of the cations are ammoniums (1096), imidazoliums (993), and pyridinums (372) based while majority of the anions are halides (1155), bistriflylimide (394), borates (168), and phosphates (168) based. The limited chemical diversity suggests a potential bias in the trained model, necessitating caution in its subsequent applications. Nevertheless, the current data set is the most comprehensive data set to the best of our knowledge.

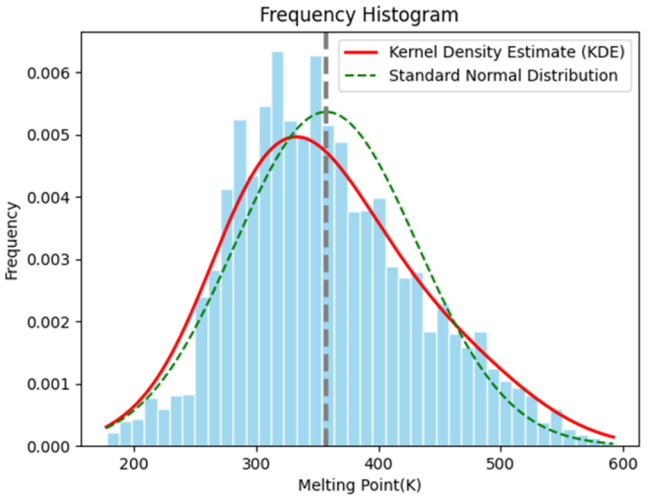

Figure 2. Distribution of the ionic liquid melting temperature in the whole data set (red line) and the standard normal distribution curve (green line).

2.2. Molecular Representation. For a predictive deep learning model in chemistry, a molecule is typically represented by an array of descriptors or a graph. One widely used molecular descriptor is the Extended Connectivity Fingerprint[34] (ECFP), which has exhibited outstanding performance in virtual screening, particularly in identifying compounds with similar bioactivity.[34] In this research, we employed ECFP4, which encodes functional groups up to two bonds away from the central atom and has demonstrated robust performance in virtual screening benchmarks.[35] The ECFP4 fingerprints were encoded as 2048-bit one-hot vector using the implementation in RDKit.[36]

Molecular descriptors, encapsulating the structural, topological, and/or physicochemical properties of molecules, have been at the core of chemo-informatics and are always the first choice in data-driven deep learning approaches.[37] As highlighted earlier, a robust model for predicting the T_m of ILs must accurately describe not only the properties of anions and cations themselves but also capture the complex and nonlinear correlations between them. Hence, Mordred[38] molecular descriptors were also employed in this work to ensure a good description of anions and cations. 1631 molecular descriptors were calculated for each anion and cation in the data set by utilizing Mordred. These molecular descriptors were then subsequently analyzed using statistical criteria to minimize the impact of multicollinearity and prevent overfitting. All columns with low variance molecular descriptors and those containing missing values or empty columns were

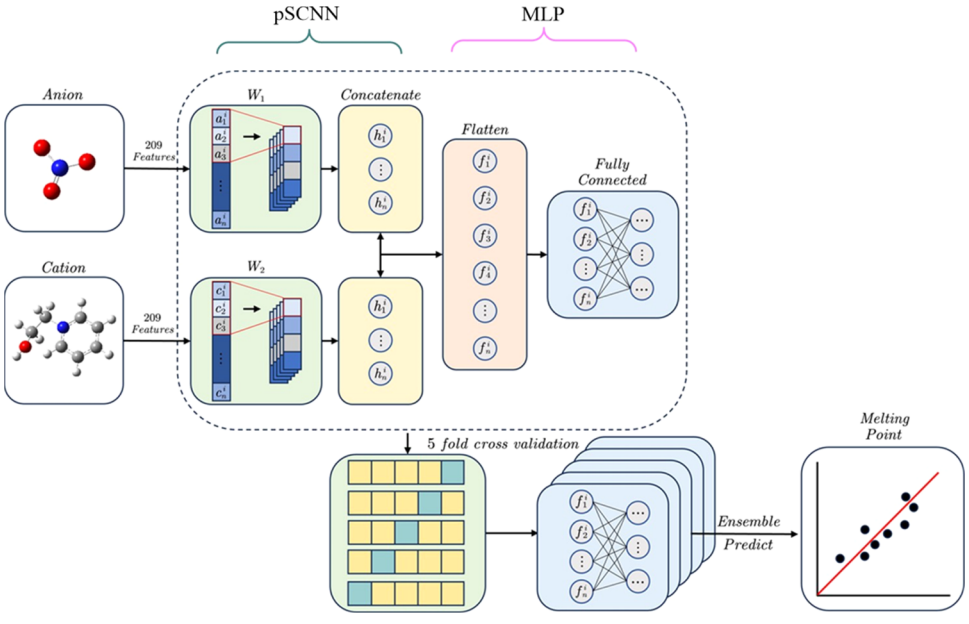

Figure 3. Schematic diagram of the proposed pSCNN model. pSCNN consists of two networks. The first one is a pseudo-Siamese convolution network for learning and extracting features of anions and cations. The extracted features are concatenated and fed into the MLP with two dense layers for prediction.

https://doi.org/10.1021/acsomega.4c02393
ACS Omega 2024, 9, 31694−31702

Table 1. Comparison of the Statistical Metrics of Different Models for Predictions of the Normal Melting Temperatures of the Ionic Liquids. For MAE and RMSE, the units are in °C

descriptors	method	N_{sample}	MAE	RMSE	R^2
ECFP4[a]	KRR[a]	2212	29.78	39.8	0.74
ECFP4 + QC[a]	KRR[a]	2212	29.15	39.5	0.74
SMILES[b]	transformer-CNF[b]	3073	27.3	35.8	0.77
	consensus model[b]	3073	26.4	34.9	0.78
ECFP4	ANN	3098	29.34	37.94	0.74
ECFP4	pSCNN	3098	29.85	38.33	0.74
mordred descriptors	ANN	3098	26.25	34.11	0.79
mordred descriptors	pSCNN	3098	24.36	31.56	0.82

[a]QC: quantum chemistry descriptors derived from quantum chemical calculations, taken from ref 24. [b]Taken from ref 27.

excluded. Pearson correlations were then applied to exclude columns with high correlation (>0.95). By excluding the molecular descriptors with low correlation (<0.05) with respect to the melting points of ILs, 178 and 47 features remained for cation and anion, respectively. Finally, the remaining features for cation and anion were combined together to keep a uniform input size as required by SCNN. In total, a set of molecular features consisting of 209 molecular descriptors for both anions and cations, were identified and used to train the pSCNN model.

2.3. Model. The pSCNN model consists of two networks as shown in Figure 3: a pseudo-Siamese convolution neural network and a fully connected multilayer perceptron (MLP). The pseudo-Siamese convolution neural network takes pairs of fingerprints or molecular descriptors as its input, which are fed into two independent subnetworks consisting of convolutional layers. Given that both anions and cations are organic/inorganic entities, these two subnetworks share identical architectures as in SCNN. However, the weights of the two networks are trained separately because anions and cations possess distinct properties and contribute differently to the melting of ILs. Through learning embeddings for input pairs, pSCNN can extract and create a feature space that maximizes the correlations between anions and cations. The learned and extracted features of anions and cations are then concatenated and fed into the MLP consisting of two dense layers for predictions, as shown in Figure 3.

For model training, the 3098 ILs were randomly split into two sets: the training set and the testing set with a ratio of 2478/620. To ensure the generalization capability of the pSCNN model, the training set was then subjected to a 5-fold cross-validation. The final prediction is then made by taking the ensemble average of five trained models from the cross-validation process. The final model developed in this study and all data used in this work are publicly available at https://github.com/Anan-Wu-XMU/pSCNN/.

2.4. Statistical Metrics. The quality of the predictive model was evaluated using the mean absolute error (MAE, eq 1), the root-mean-square error (RMSE, eq 2), and the squared coefficient of correlation (R^2, eq 3).

$$\mathrm{MAE} = \frac{1}{n}\sum_{i=1}^{n} |y_{\mathrm{pred},i} - y_{\mathrm{exp},i}| \quad (1)$$

$$\mathrm{RMSE} = \sqrt{\frac{1}{n}\sum_{i}^{n} (y_{\mathrm{pred},i} - y_{\mathrm{exp},i})^2} \quad (2)$$

$$R^2 = 1 - \frac{\sum_{i}^{n} (y_{\mathrm{pred},i} - y_{\mathrm{exp},i})^2}{\sum_{i}^{n} (y_{\mathrm{pred},i} - \overline{y_{\mathrm{exp}}})^2} \quad (3)$$

where n is the number of ionic liquids, y_{exp} is the experimental T_m, y_{pred} is the predicted T_m, and $\overline{y_{\mathrm{exp}}}$ is the mean values of all experimental T_m in the set.

3. RESULTS AND DISCUSSION

3.1. Model Performance. The melting process of ILs is intricate and is still not well understood. However, certain facts are known: (1) both intramolecular and intermolecular factors are pivotal in the melting process; (2) van der Waals and electrostatic interactions assume distinct roles for different kinds of ILs; (3) Nonlinear entropy effects complicate the prediction of the T_m of ILs. Previous investigations have demonstrated that ANN can effectively handle complex nonlinear problem by correlating input features.[39,40] Hence, the ANN models are included in this study for comparison. A summary of the performance of various models is presented in Table 1.

For the KRR model based on ECFP4 reported by Low et al., the MAE and RMSE are 29.78 and 39.8 °C, respectively, with a moderate R^2 of 0.74 (Table 1). The introduction of quantum chemical descriptors, intended to describe the interion interactions, yields only a slightly improved result, with MAE decreasing from 29.78 to 29.15 °C. However, using the same ECFP4 as descriptors, the deep learning models (ANN and pSCNN) do not outperform the conventional machine learning method as expected, even with a larger data set. For instance, ANN and pSCNN predict the T_m of ILs with MAEs of 29.34 and 29.85 °C, respectively (Table 1). Although DLs have generated various important breakthroughs in many areas, it is known that they are not friendly designed for application involving high-dimensional sparse data.[41] Given the often sparse and highly dimensional nature of ECFP4, it is not surprising that both ANN and pSCNN do not outperform the conventional machine learning method in predicting the T_m of ILs using ECFP4 as descriptors. A closer inspection reveals that the feature space of halogen anions represented by ECFP4 is extremely sparse, with only 1 out of 2048 dimensions being nonzero. Since halogen anions are widely present in ILs (1155/3098), this will inevitably lead to the notorious "curse of dimensionality" in DLs,[42] resulting in unsatisfied generalization performance, as shown above. Other molecular representations that do not generate sparse features (such as Mordred molecular descriptors) may yield better results.

The results of the ANN model using Mordred descriptors as input did improve compared to the ANN model based on the

https://doi.org/10.1021/acsomega.4c02393
ACS Omega 2024, 9, 31694−31702

ECFP4 fingerprint. Its test MAE, RMSE, and R^2 are 26.25, 34.11 °C, and 0.79, respectively, outperforming the best model in the literature (Table 1, Transformer-CNF). As reported by Makarov et al.,[27] the Transformer-CNF model relies only on the augmented SMILES and can achieve the best accuracy among all general models reported to date (Table 1, i.e., MAE: 27.3, RMSE: 35.8 °C and R^2: 0.77). As stated in Section 1, a robust model for predicting the T_m of ILs not only needs to accurately describe the properties of anions and cations themselves but also needs to describe the complex and nonlinear correlations between anions and cations. Transformer-CNF meets the above conditions to a certain extent. On the one hand, Transformer can effectively extract encoded chemical information from SMILES, allowing it to describe the properties of individual ions well. On the other hand, the intrinsic attention mechanism in the Transformer architecture can describe the correlation between anions and cations to a certain extent. However, systematic investigations[43] show that the number of augmented SMILES plays a decisive role in the results, and it usually requires 20+ augmentations to achieve good enough results. 10-fold augmentation adopted by Makarov et al. may be insufficient.

In comparison to ANNs and transformer-based methods, SCNN is designed to learn and extract features from pairs of input samples and make decisions based on their correlation.[29] Therefore, SCNN is particularly suitable for predicting the T_m of ILs provided that the properties of single ions can be well described. Using Mordred descriptors as input features, it is encouraging to see from Table 1 and Figure 4 that our pSCNN

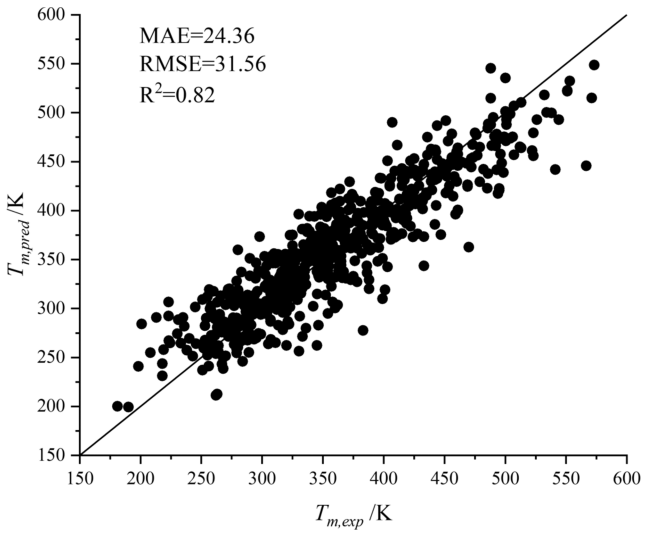

Figure 4. Parity plot comparing the predicted melting point values ($T_{m,pred}$) with the corresponding experimental values ($T_{m,exp}$).

model has had the best accuracy so far. The introduction of the Siamese network does help to better learn and extract features from pairs of input samples as desired. The MAE and RMSE are significantly reduced from 26.25 and 34.11 °C (ANN/Mordred: Table 2) to 24.36 and 31.56 °C, respectively. The R^2 value of 0.82 is one of the highest values among all general models (Table 1). This superior performance highlights the importance of choosing the proper model that matches the nature of the problem.

3.2. Applicability Domain Analysis. For a predictive model, applicability domain analysis (ADAN) is also a crucial aspect to assess the reliability of the mode.[44] To establish the boundaries within which the model predictions can be trusted, a probability-based and distance-oriented algorithm was applied. The query compound is considered as an outlier, and the prediction is marked as unreliable when the calculated average Euclidean distance with respect to the training set falls outside the 95% confidence interval boundary.

Figure 5 shows the applicability domain analysis for the pSCNN model, wherein the reliable prediction space is obtained by computing the 95 and 99% confidence interval boundaries. In the testing set, our analysis demonstrated that 34 ILs were outside the 95% confidence interval boundary (Figure 5, points in orange and red) with 7 ILs outside the 99% confidence interval boundary (Figure 5, points in red). Thus, the pSCNN model could account for nearly 95% reliable predictions across 620 compounds in the testing set. Such a performance is already satisfactory on the blind test.

Upon close inspection of the ILs for which predictions were flagged as unreliable, it was revealed that these ILs contained cations or anions that were highly underrepresented in the calibration, and a majority of these ILs (25 out of 34) were even new ILs (Table S2). These ILs represent a significant challenge for melting point predictions. In such a stringent test, it is encouraging to see that our model can still produce reasonable predictions with MAE and RMSE of 30.4 and 37.0 °C, respectively. This suggests that by learning and extracting features from input pairs, our model has good generalization capability in predicting the T_m of ILs. In fact, this validation on outliers corresponds to the most rigorous "compounds out" adopted by Makarov et al.,[26,27] both indicating the predictive power of the model for ionic liquids with novel ions. If the model is applied to predicting only a new combination of ions, the pSCNN model is expected to provide more accurate results. Thus, it may provide a simple yet efficient way to help experimentalists in advancing and customizing the synthesis of new IL. Note that predicting the T_m of a new IL by using the pSCNN model (including the feature generation) will take an average of 1.02 s on a workstation made of dual processor Intel Xeon Silver 4110@2.10 GHz.

3.3. Feature Importance. While the melting process of ILs is not fully understood, it is well recognized that factors primarily controlling the T_m of an ionic liquid include intermolecular forces (van der Waals and electrostatic), molecular symmetry, and the conformational degrees of freedom of a molecule.[45]

To further examine whether our model captures the essence of the problem being addressed, we analyzed feature importance based on permutation importance (see the Supporting Information (SI) for more information). Figure 6 shows the top 10 most important molecular descriptors that have a significant impact on T_m of ILs. Notably, all key features (Figure 6) are molecular descriptors related to either topological characters (IC3, IC2, IC5, and AATS0v) or electrostatic characters (PEOE_VSA7, VSA_Estat8, PEOE_VSA12, PEOE_VSA13, SlogP_VSA8, and Xc-3d). As the most important descriptors, ICx (IC3, IC2, and IC5) describe the connectivity and branching in the molecule. They are closely related to molecular shape and local symmetry, thus having a profound effect on the T_m of ILs. PEOE_VSAx (PEOE_VSA7, PEOE_VSA12, and PEOE_VSA13), on the other hand, quantify the van der Waals surface area of molecules with a specific charge range, aiming to capture direct electrostatic interactions[46] that influence the T_m of ILs. SlogP_VSA8 is

https://doi.org/10.1021/acsomega.4c02393
ACS Omega 2024, 9, 31694−31702

Table 2. Predicted Melting Points for 39 Newly Synthesized Ionic Liquids[a]

name	$T_{m,exp}$[b]	$T_{m,pred(transformerCNN)}$[c]	$T_{m,pred(transformerCNF)}$[d]	$T_{m,pred(pSCNN)}$
1-butyl-3-methylimidazolium hydrogen sulfate	293	311	300	293.4
1-ethyl-3-methylimidazolium hydrogen sulfate	300	296	280	277.1
N-methyl-*N*-propylpyrrolidinium acetate	289.8	291	310	280.4
N-ethyl-*N*-methylmorpholinium bromide	445.6	413	440	420.5
1-butyl-3-methylimidazolium bromide	352.1	315	330	346.1
1-butyl-3-methylimidazolium trifluoromethanesulfonate	291.1	300	290	294.3
1-butyl-1-methylpiperidinium trifluoromethanesulfonate	309.1	330	350	348.6
1-butylpyridinium chloride	405.4	357	350	366.9
1-(2-Methoxyethyl)-1-methylpyrrolidinium hexafluorophosphate	307	311	300	313.1
1-butyl-1-methylpyrrolidinium bis(fluorosulfonyl)amide	253.5	288	270	277.2
1-ethyl-3-methylimidazolium bromide	350.2	354	360	348.6
1-butyl-3-methylpyridinium hexafluorophosphate	324.8	331	350	323.1
1-butyl-1-methylpiperidinium hexafluorophosphate	354.7	403	400	405.7
1-butyl-1-methylpyrrolidinium hexafluorophosphate	359.7	393	380	364.6
1-(2-hydroxyethyl)-3-methylimidazolium nonafluoro-1-butanesulfonate	251.5	293	280	322.4
1-(2-hydroxyethyl)-3-methylimidazolium perfluoropentanoate	294.8	271	280	285.0
1-ethyl-4-methylpyridinium bis((trifluoromethyl)sulfonyl)amide	288	298	290	287.4
1-ethyl-2-methylpyridinium bis((trifluoromethyl)sulfonyl)amide	289	281	290	293.4
N-(3-cyanopropyl)pyridinium tricyanomethanide	305.2	313	330	303.0
choline tosylate	378.1	393	380	389.8
1-ethylpyridinium 4-methylbenzenesulfonate	374.1	350	350	368.9
1-butyl-3-methylimidazolium bis(trifluoromethylsulfonyl)imide	266.6	263	250	266.8
1-ethyl-3-methylimidazolium bis((trifluoromethyl)sulfonyl)imide	256	268	260	261.8
1-ethyl-3-methylimidazolium trifluoromethanesulfonate	262.6	299	270	270.9
1-ethyl-3-methylimidazolium 4-methylbenzenesulfonate	328.2	349	350	338.5
1-ethyl-3-methylimidazolium thiocyanate	266	283	280	276.4
1-ethyl-3-methyl-1*H*-imidazolium tricyanomethanide	274.9	274	270	281.2
1-ethyl-3-methylimidazolium dimethylphosphate	312.9	280	270	306.0
tetrabutylphosphonium bromide	376.1	370	380	393.5
1-ethyl-3-methylimidazolium bis((trifluoromethyl)sulfonyl)imide	259.1	268	260	260.6
1-ethyl-3-methylimidazolium tetrafluoroborate	284.1	270	270	281.5
N,*N*,*N*-triethylhexan-1-aminium trifluoromethanesulfonate	347.83	319	330	351.8
N,*N*,*N*-triethylhexan-1-aminium tricyanomethanide	290.03	270	280	300.1
N-decyl-*N*-methylmorpholinium trifluoromethanesulfonate	349.2	350	340	353.9
3-ethylthiazolium bis((trifluoromethyl)sulfonyl)amide	303.1	303	300	324.5
cetylpyridinium chloride	354.1	343	340	364.5
1-hexadecyl-1-methylpiperidinium acetylsalicylate	303.9	309	310	350.3
1-hexadecyl-1-methylpiperidinium chloride	365.9	393	390	374.1
3-methyl-1-octadecyl-1*H*-imidazolium bis((trifluoromethyl)sulfonyl)amide	328.1	306	300	318.0
MAE		17.8	16.3	13.4
RMSE		22.4	20.9	20.6

[a]Units are in Kelvin (K). [b]Taken from ref 11. [c]Evaluated with the model in ref 26. [d]Evaluated with the model in ref 27.

designed to capture the hydrophobic or lipophilic properties of a molecule,[46] which is directly related to intermolecular van der Waals interactions and thus affects the melting point of the ionic liquid.

All of these results clearly demonstrate that our pSCNN model, by learning and extracting features from pairs of input, indeed captures the essence of the problem being addressed. Thus, it can provide an accurate yet efficient way to predict the T_m of ILs.

3.4. External Validation and Perspective. Over the past few years, new data have continuously emerged in the journals and monographs. To further check the generalization performance of our pSCNN model, an independent test was conducted using 39 newly synthesized ILs, sourced from NIST ILThermo database.[11] These ILs did not overlap with the ILs used in the development of the model. Results of the Transformer-CNF models were included for comparison.

ADAN (Figure S1) reveals that all 39 ILs are within the 95% confidence interval boundary, indicating that they should have good prediction results. The evaluations by our model indeed produced excellent results, with MAE and RMSE of 13.4 and 20.6 °C, respectively. These results are clearly superior to the two Transformer-CNF models[26,27] with MAE and RMSE of 17.8, 22.4 °C and 16.3, 20.9 °C respectively (Table 2).

Detailed analysis showed that the majority of the prediction errors (23 out of 39) were less than 10 °C, which is an encouraging result for the design of new ILs. Large errors mainly occur when the occurrence rate of cations or anions is low. For instance, the largest error (71 °C, Table 2) was calculated for 1-(2-hydroxyethyl)-3-methylimidazolium nonafluoro-1-butanesulfonate, in which the 1-(2-hydroxyethyl)-3-methylimidazolium occurs only twice in the calibration. The cause of this high error may also be due to the fact that

https://doi.org/10.1021/acsomega.4c02393
ACS Omega 2024, 9, 31694−31702

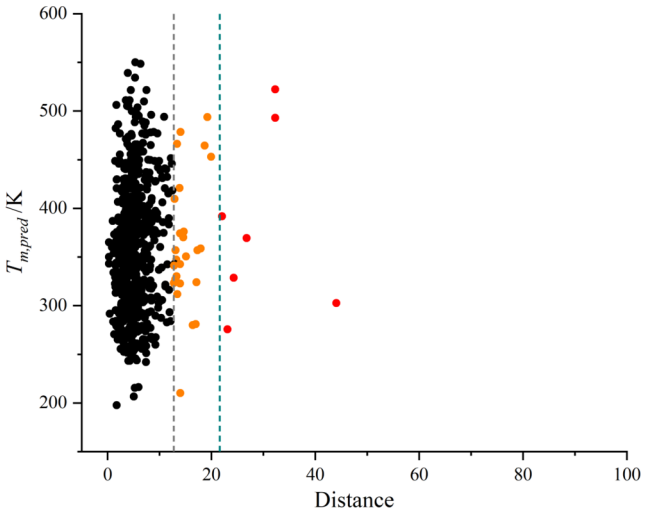

Figure 5. Boundaries of the applicability domain for the pSCNN model. Compounds positioned to the left of the gray dashed line fall within the 95% confidence interval, while those positioned to the left of the green dashed line are within the 99% confidence interval.

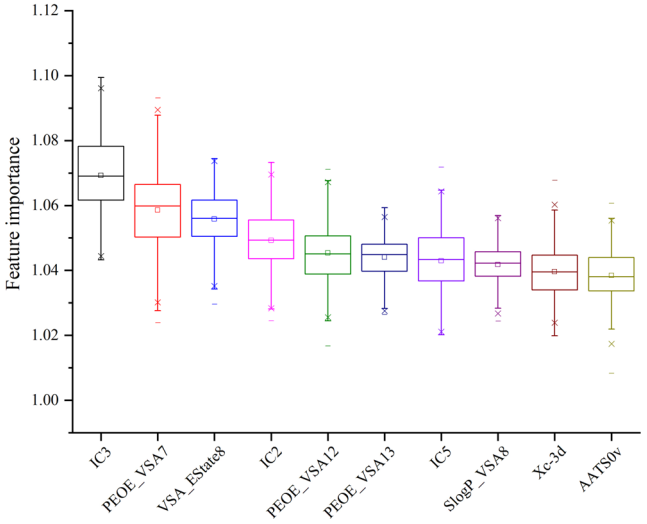

Figure 6. Top 10 most important molecular descriptors that have a significant impact on the T_m of ILs.

experimental measurements for ILs with very high (>200 °C) and low (<0 °C) T_m are often prone to errors.[47]

These results further strengthened the argument that, by learning and extracting features from pairs of input, the pSCNN model indeed captures the essence of the problem being addressed and hence can predict the T_m of ILs with good accuracy.

Considering that the synthesis of an ionic liquid is generally challenging and time-consuming, and the number of ionic liquids is virtually unlimited, it is therefore crucial to narrow down the potential pool of suitable ionic liquids to be synthesized. By taking combinations of all cations (1760) and anions (203) in our data set, we could evaluate the T_m of nearly 360,000 ILs (Figure 7) with satisfactory accuracy using our pSCNN model. This extensive data set, with diverse T_m's ranging from −100 to 367 °C, may provide immense value for advancing and customizing the synthesis of new IL.

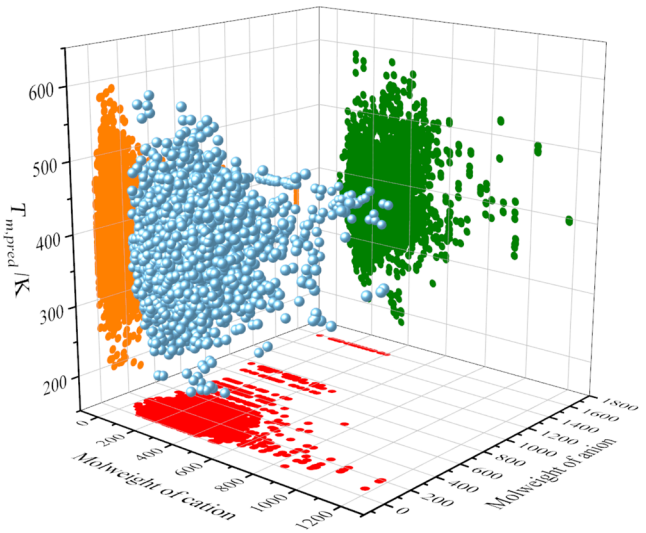

Figure 7. Predicted melting points of all potential ILs generated by the pSCNN model.

4. CONCLUSIONS

Ionic liquids (IL) offer a broad spectrum of potential applications, owing to their distinctive and tunable properties, rendering them versatile across diverse fields. However, the practical applications of numerous ionic liquids are often constrained by their unfavorable physical or chemical properties. Due to the extensive number of potential combinations of anions and cations, the experimental screening of ionic liquids is impractical. Consequently, a robust and efficient method for predicting the properties of ionic liquids becomes imperative. In this study, we focused on predicting the normal melting temperature of ionic liquids, employing a pseudo-Siamese convolution neural network (pSCNN) inspired by SCNN. Utilizing a comprehensive data set of 3098 ILs, comprising 203 distinct anions and 1760 unique cations, we systematically assess various deep learning models (ANN, pSCNN, and Transformer-CNN), along with molecular descriptors (ECFP fingerprint and Mordred properties), for their performance in predicting the T_m of ILs. Noteworthy among the investigated modeling schemes, the pSCNN, in conjunction with filtered Mordred descriptors, demonstrates superior performance, yielding a mean absolute error (MAE) and root-mean-square error (RMSE) of 24.36 and 31.56 °C, respectively.

Subsequent feature analysis uncovered that the pivotal molecular descriptors influencing the melting process of ionic liquids are intricately associated with molecular symmetry, electrostatic interactions, and van der Waals forces. This observation highlights the effectiveness of the pSCNN model, which, by learning and extracting features from input pairs, effectively captures the essence of the addressed problem, explaining its superior performance. It is noteworthy that the same methodology can be extended to predict various other properties of ionic liquids.

By applying the pSCNN model to all combinations of anions and cations within our data set, we constructed an extensive database for advancing and customizing the synthesis of new IL. The final model developed in this study and all data used in this work are publicly available at https://github.com/Anan-Wu-XMU/pSCNN/.

https://doi.org/10.1021/acsomega.4c02393
ACS Omega 2024, 9, 31694−31702

■ ASSOCIATED CONTENT

Data Availability Statement

All materials for the prediction of the normal melting point of ionic liquid are publicly available at https://github.com/Anan-Wu-XMU/pSCNN/.

Supporting Information

The Supporting Information is available free of charge at https://pubs.acs.org/doi/10.1021/acsomega.4c02393.

Selected models for IL melting point prediction (Table S1); brief description of permutation feature importance analysis; T_m of ILs lay outside the 95% confidence interval boundary (Table S2); and boundaries of the applicability domain for the 39 ILs (Figure S1) (PDF)

■ AUTHOR INFORMATION

Corresponding Authors

Anan Wu − *State Key Laboratory of Physical Chemistry of Solid Surface, Fujian Provincial Key Laboratory for Theoretical and Computational Chemistry, Departmental of Chemistry, College of Chemistry and Chemical Engineering, Xiamen University, Xiamen 361005, P. R. China;* orcid.org/0000-0001-5243-9291; Email: ananwu@xmu.edu.cn

Xin Lu − *State Key Laboratory of Physical Chemistry of Solid Surface, Fujian Provincial Key Laboratory for Theoretical and Computational Chemistry, Departmental of Chemistry, College of Chemistry and Chemical Engineering, Xiamen University, Xiamen 361005, P. R. China;* orcid.org/0000-0003-4968-9462; Email: xinlu@xmu.edu.cn

Authors

Tao Liang − *State Key Laboratory of Physical Chemistry of Solid Surface, Fujian Provincial Key Laboratory for Theoretical and Computational Chemistry, Departmental of Chemistry, College of Chemistry and Chemical Engineering, Xiamen University, Xiamen 361005, P. R. China*

Wei Liu − *State Key Laboratory of Physical Chemistry of Solid Surface, Fujian Provincial Key Laboratory for Theoretical and Computational Chemistry, Departmental of Chemistry, College of Chemistry and Chemical Engineering, Xiamen University, Xiamen 361005, P. R. China*

Kai Tan − *State Key Laboratory of Physical Chemistry of Solid Surface, Fujian Provincial Key Laboratory for Theoretical and Computational Chemistry, Departmental of Chemistry, College of Chemistry and Chemical Engineering, Xiamen University, Xiamen 361005, P. R. China;* orcid.org/0000-0001-8372-2778

Complete contact information is available at: https://pubs.acs.org/10.1021/acsomega.4c02393

Notes

The authors declare no competing financial interest.

■ ACKNOWLEDGMENTS

This work was supported by the National Natural Science Foundation of China (nos. 92161117 and 22373079) and the Natural Science Foundation of Fujian Province of China (grant no. 2021J01020).

■ REFERENCES

(1) Freemantle, M. *An Introduction to Ionic Liquids*; Royal Society of Chemistry, 2010.

(2) Lei, Z. G.; Dai, C. N.; Chen, B. H. Gas Solubility in Ionic Liquids. *Chem. Rev.* **2014**, *114* (2), 1289−1326.

(3) Watanabe, M.; Thomas, M. L.; Zhang, S. G.; Ueno, K.; Yasuda, T.; Dokko, K. Application of Ionic Liquids to Energy Storage and Conversion Materials and Devices. *Chem. Rev.* **2017**, *117* (10), 7190−7239.

(4) Zhang, Q. H.; Zhang, S. G.; Deng, Y. Q. Recent advances in ionic liquid catalysis. *Green Chem.* **2011**, *13* (10), 2619−2637.

(5) Zhou, Y.; Qu, J. Ionic Liquids as Lubricant Additives: A Review. *Acs Appl. Mater. Interfaces* **2017**, *9* (4), 3209−3222.

(6) Sahbaz, Y.; Williams, H. D.; Nguyen, T. H.; Saunders, J.; Ford, L.; Charman, S. A.; Scammells, P. J.; Porter, C. J. H. Transformation of Poorly Water-Soluble Drugs into Lipophilic Ionic Liquids Enhances Oral Drug Exposure from Lipid Based Formulations. *Mol. Pharmaceutics* **2015**, *12* (6), 1980−1991.

(7) Gupta, K. M.; Jiang, J. W. Cellulose dissolution and regeneration in ionic liquids: A computational perspective. *Chem. Eng. Sci.* **2015**, *121*, 180−189.

(8) Hijo, A. A. C. T.; Maximo, G. J.; Costa, M. C.; Batista, E. A. C.; Meirelles, A. J. A. Applications of Ionic Liquids in the Food and Bioproducts Industries. *Acs Sustainable Chem. Eng.* **2016**, *4* (10), 5347−5369, DOI: 10.1021/acssuschemeng.6b00560.

(9) Zhang, J.; Sun, B.; Zhao, Y.; Tkacheva, A.; Liu, Z.; Yan, K.; Guo, X.; McDonagh, A. M.; Shanmukaraj, D.; Wang, C.; et al. A versatile functionalized ionic liquid to boost the solution-mediated performances of lithium-oxygen batteries. *Nat. Commun.* **2019**, *10* (1), No. 602.

(10) Hallett, J. P.; Welton, T. Room-Temperature Ionic Liquids: Solvents for Synthesis and Catalysis. 2. *Chem. Rev.* **2011**, *111* (5), 3508−3576.

(11) https://ilthermo.boulder.nist.gov/.

(12) Katritzky, A. R.; Lomaka, A.; Petrukhin, R.; Jain, R.; Karelson, M.; Visser, A. E.; Rogers, R. D. QSPR correlation of the melting point for pyridinium bromides, potential ionic liquids. *J. Chem. Inf. Comput. Sci.* **2002**, *42* (1), 71−74.

(13) Izgorodina, E. I.; Seeger, Z. L.; Scarborough, D. L. A.; Tan, S. Y. S. Quantum Chemical Methods for the Prediction of Energetic, Physical, and Spectroscopic Properties of Ionic Liquids. *Chem. Rev.* **2017**, *117* (10), 6696−6754.

(14) Sun, N.; He, X. Z.; Dong, K.; Zhang, X. P.; Lu, X. M.; He, H. Y.; Zhang, S. J. Prediction of the melting points for two kinds of room temperature ionic liquids. *Fluid Phase Equilib.* **2006**, *246* (1−2), 137−142.

(15) López-Martin, I.; Burello, E.; Davey, P. N.; Seddon, K. R.; Rothenberg, G. Anion and cation effects on imidazolium salt melting points: A descriptor modelling study. *ChemPhysChem* **2007**, *8* (5), 690−695.

(16) Huo, Y.; Xia, S. Q.; Zhang, Y.; Ma, P. S. Group Contribution Method for Predicting Melting Points of Imidazolium and Benzimidazolium Ionic Liquids. *Ind. Eng. Chem. Res.* **2009**, *48* (4), 2212−2217.

(17) Gharagheizi, F.; Ilani-Kashkouli, P.; Mohammadi, A. H. Computation of normal melting temperature of ionic liquids using a group contribution method. *Fluid Phase Equilib.* **2012**, *329*, 1−7.

(18) Mital, D. K.; Nancarrow, P.; Ibrahim, T. H.; Jabbar, N. A.; Khamis, M. I. Ionic Liquid Melting Points: Structure-Property Analysis and New Hybrid Group Contribution Model. *Ind. Eng. Chem. Res.* **2022**, *61* (13), 4683−4706.

(19) Varnek, A.; Kireeva, N.; Tetko, I. V.; Baskin, I. I.; Solov'ev, V. P. Exhaustive QSPR studies of a large diverse set of ionic liquids: How accurately can we predict melting points? *J. Chem. Inf. Model.* **2007**, *47* (3), 1111−1122.

(20) Varnek, A.; Baskin, I. Machine Learning Methods for Property Prediction in Chemoinformatics:? *J. Chem. Inf. Model.* **2012**, *52* (6), 1413−1437.

(21) Wu, A.; Ye, Q.; Zhuang, X.; Chen, Q.; Zhang, J.; Wu, J.; Xu, X. Elucidating Structures of Complex Organic Compounds Using a Machine Learning Model Based on the 13C NMR Chemical Shifts. *Precis. Chem.* **2023**, *1* (1), 57−68.

(22) Carrera, G.; Aires-de-Sousa, J. Estimation of melting points of pyridinium bromide ionic liquids with decision trees and neural networks. *Green Chem.* **2005**, *7* (1), 20−27.
(23) Venkatraman, V.; Evjen, S.; Knuutila, H. K.; Fiksdahl, A.; Alsberg, B. K. Predicting ionic liquid melting points using machine learning. *J. Mol. Liq.* **2018**, *264*, 318−326.
(24) Low, K.; Kobayashi, R.; Izgorodina, E. I. The effect of descriptor choice in machine learning models for ionic liquid melting point prediction. *J. Chem. Phys.* **2020**, *153* (10), No. 104101, DOI: 10.1063/5.0016289.
(25) Baskin, I.; Epshtein, A.; Ein-Eli, Y. Benchmarking machine learning methods for modeling physical properties of ionic liquids. *J. Mol. Liq.* **2022**, *351*, No. 118616, DOI: 10.1016/j.molliq.2022.118616.
(26) Makarov, D. M.; Fadeeva, Y. A.; Shmukler, L. E.; Tetko, I. V. Beware of proper validation of models for ionic Liquids! *J. Mol. Liq.* **2021**, *344*, No. 117722, DOI: 10.1016/j.molliq.2021.117722.
(27) Makarov, D. M.; Fadeeva, Y. A.; Shmukler, L. E.; Tetko, I. V. Machine learning models for phase transition and decomposition temperature of ionic liquids. *J. Mol. Liq.* **2022**, *366*, No. 120247, DOI: 10.1016/j.molliq.2022.120247.
(28) Valderrama, J. O.; Faúndez, C. A.; Vicencio, V. J. Artificial Neural Networks and the Melting Temperature of Ionic Liquids. *Ind. Eng. Chem. Res.* **2014**, *53* (25), 10504−10511.
(29) Nandy, A.; Haldar, S.; Banerjee, S.; Mitra, S. In *A Survey on Applications of Siamese Neural Networks in Computer Vision*, In Proceedings of the 2020 International Conference for Emerging Technology (INCET), Belgaum, India, 5−7 June; IEEE, 2020; pp 1−5.
(30) Koch, G.; Zemel, R.; Salakhutdinov, R. In *Siamese Neural Networks for One-Shot Image Recognition*, Proceedings of the 32nd International Conference on Machine Learning; JMLR, 2015.
(31) Wei, W. W.; Liao, Y. X.; Wang, Y. F.; Wang, S. Q.; Du, W.; Lu, H. M.; Kong, B.; Yang, H. W.; Zhang, Z. M. Deep Learning-Based Method for Compound Identification in NMR Spectra of Mixtures. *Molecules* **2022**, *27* (12), No. 3653, DOI: 10.3390/molecules27123653.
(32) Fernández-Llaneza, D.; Ulander, S.; Gogishvili, D.; Nittinger, E.; Zhao, H.; Tyrchan, C. Siamese Recurrent Neural Network with a Self-Attention Mechanism for Bioactivity Prediction. *Acs Omega* **2021**, *6* (16), 11086−11094.
(33) McKinney, W. In *Data Structures for Statistical Computing in Python*, Proceedings of the 9th Python in Science Conference; van der Walt, S.; Millman, J., Eds.; 2010; pp 56−61.
(34) Rogers, D.; Hahn, M. Extended-Connectivity Fingerprints. *J. Chem. Inf. Model.* **2010**, *50* (5), 742−754.
(35) Riniker, S.; Landrum, G. A. Open-source platform to benchmark fingerprints for ligand-based virtual screening. *J. Cheminf.* **2013**, *5*, No. 26, DOI: 10.1186/1758-2946-5-26.
(36) Landrum, G. rdkit: Open-Source Cheminformatics 2023. http://www.rdkit.org.
(37) Fernández-Torras, A.; Comajuncosa-Creus, A.; Duran-Frigola, M.; Aloy, P. Connecting chemistry and biology through molecular descriptors. *Curr. Opin. Chem. Biol.* **2022**, *66*, No. 102090, DOI: 10.1016/j.cbpa.2021.09.001.
(38) Moriwaki, H.; Tian, Y. S.; Kawashita, N.; Takagi, T. Mordred: a molecular descriptor calculator. *J. Cheminf.* **2018**, *10*, No. 4, DOI: 10.1186/s13321-018-0258-y.
(39) Almeida, J. S. Predictive non-linear modeling of complex data by artificial neural networks. *Curr. Opin. Biotechnol.* **2002**, *13* (1), 72−76, DOI: 10.1016/S0958-1669(02)00288-4.
(40) LeCun, Y.; Bengio, Y.; Hinton, G. Deep learning. *Nature* **2015**, *521*, 436−444.
(41) Jiang, B. Y.; Deng, C.; Yi, H. M.; Hu, Z. L.; Zhou, G. R.; Zheng, Y.; Huang, S.; Guo, X. Y.; Wang, D. Y.; Song, Y.et al. In *XDL: An Industrial Deep Learning Framework for High-dimensional Sparse Data*, 1st International Workshop on Deep Learning Practice for High-Dimensional Sparse Data with Kdd (Dlp-Kdd 2019); ACM Digital Library, 2019.
(42) Altman, N.; Krzywinski, M. The curse(s) of dimensionality. *Nat. Methods* **2018**, *15* (6), 399−400.
(43) Tetko, I. V.; Karpov, P.; Van Deursen, R.; Godin, G. State-of-the-art augmented NLP transformer models for direct and single-step retrosynthesis. *Nat. Commun.* **2020**, *11*, No. 5575, DOI: 10.1038/s41467-020-19266-y.
(44) Carrió, P.; Pinto, M.; Ecker, G.; Sanz, F.; Pastor, M. Applicability Domain Analysis (ADAN): A Robust Method for Assessing the Reliability of Drug Property Predictions. *J. Chem. Inf. Model.* **2014**, *54* (5), 1500−1511.
(45) Katritzky, A. R.; Jain, R.; Lomaka, A.; Petrukhin, R.; Maran, U.; Karelson, M. Perspective on the relationship between melting points and chemical structure. *Cryst. Growth Des.* **2001**, *1* (4), 261−265.
(46) Labute, P. A widely applicable set of descriptors. *J. Mol. Graphics Model.* **2000**, *18* (4−5), 464−477.
(47) Tetko, I. V.; Lowe, D. M.; Williams, A. J. The development of models to predict melting and pyrolysis point data associated with several hundred thousand compounds mined from PATENTS. *J. Cheminf.* **2016**, *8*, No. 2, DOI: 10.1186/s13321-016-0113-y.

https://doi.org/10.1021/acsomega.4c02393
ACS Omega 2024, 9, 31694−31702